Materials Research. 2017; 20(2): 430-435
DOI: http://dx.doi.org/10.1590/1980-5373-MR-2016-0628

Characterization of *Sn* Doped *ZnS* Thin Films Synthesized by CBD

Ayan Mukherjee[a], Partha Mitra[a]*

[a]Department of Physics, The University of Burdwan, Burdwan, 713104, India

Received: August 31, 2016; Revised: November 10, 2016; Accepted: January 02, 2017.

Zinc sulphide (*ZnS*) thin film were prepared using chemical bath deposition (CBD) process and tin (*Sn*) doping was successfully carried out in *ZnS*. Structural, morphological and microstructural characterization was carried out using XRD, TEM, FESEM and EDX. XRD and SAED pattern confirms presence of hexagonal phase. Reitveld analysis using MAUD software was used for particle size estimation. A constantly decreasing trend in particle size was observed with increasing tin incorporation in *ZnS* film which was due to enhanced microstrain resulting for tin incorporation. The particle size of prepared hexagonal wurtzite *ZnS* was around 14-18 nm with average size of ~16.5 nm. The bandgap of the film increases from ~ 3.69 eV for *ZnS* to ~ 3.90 eV for 5% *Sn* doped *ZnS* film which might be due to more ordered hexagonal structure as a result of tin incorporation. Band gap tenability property makes *Sn* doped *ZnS* suitable for application in different optoelectronics devices. PL study shows variation of intensity with excitation wavelength and a red shift is noticed for increasing excitation wavelength.

Keywords: *CBD, Sn:ZnS thin film, XRD, TEM, Particle size, Optical band gap*

1. Introduction

Zinc sulfide *ZnS* is one of the direct II–VI semiconductor compounds with large band gap energy of ~3.65 eV at room temperature[1].The material crystallizes in both cubic and hexagonal forms and is a material of reference to test several theoretical models in condensed matter physics[2]. Sometimes it shows mixed phase crystal structure. While cubic *ZnS* has been reported to have a wide direct bandgap of ~3.6 eV at 300K, hexagonal *ZnS* has been reported to have a bandgap of ~ 3.91 eV[3]. The material has huge potential application in both bulk and thin film form in various photovoltaic and optoelectronic devices[4].It is used as key material for solar control coating, optoelectronic devices, electroluminescence devices, sensors and others[5]. *ZnS* is a prospective material to be used in solar cell as passivation layer for better photovoltaic properties[6]. Due to its high refractive index ($n \sim 2.3$), it can be used as an antireflective coating[7]. *ZnS* is alsoan important phosphor host lattice material used in electroluminescent devices (ELD). This is because of its large band gap that is enough to emit visible light without absorption and the efficient transport of high energy electrons[8].Various physical and chemical techniques have been used by researchers to deposit *ZnS* thin films. While physical deposition methods such as sputtering, metal organic chemical vapor deposition (MOCVD), molecular beam epitaxy (MBE) and atomic layer epitaxy (ALE) demand the use of either vacuum conditions and/or complex equipment, chemical techniques are simpler and cost effective. Thus they have become more popular in recent times. Various chemical techniques that has been used includes electrodeposition[9], spray pyrolysis[10-11], sol-gel[1], spin coating[5] and chemical bath deposition[12-15] etc. The technique of CBD (also known as chemical solution deposition) is simple, inexpensive and can be adaptable to large area processing with low fabrication cost. Also doping with metal ions at low temperatures can be conveniently carried out at this technique. Doping of *ZnS* with group II metal ions has been made to achieve improved electrical and optical properties. Copper doping has been reported to strongly influence resistivity and band gap[16-17]. Increase of Cu^{2+} concentration has been reported to result in quenching of luminescence due to formation of *CuS*[18]. Doping with *Mn* has been reported to give highly transparent *ZnS* film along with quantum size effect[19]. Quantum confinement was also reported *Mn* doped *ZnS* thin films prepared by spin coating[5]. Strong luminescence band at energy 2.07 eV has been reported for *Mn* doped *ZnS* prepared by wet chemical technique[20]. Doping of transition metal ions of copper and manganese has been reported to show intense, stable and tunable emission covering the blue to red end of visible spectrum[21]. As *ZnS* radiates luminescence with a wavelength 420-480 nm, copper and manganese has been doped to order to receive radiation in the visible region. Although influence of *Cu* and *Mn* on physical properties of *ZnS* has been reported by several researchers, influence of tin incorporation in *ZnS* thin film is almost nonexisting.

* e-mail: mitrapartha1@rediffmail.com

For tin doped *ZnS* nanoparticles with thiourea as capping agent, quantum confinement effect leading to blue shift in band gap has been reported[18]. Detail information regarding effect of tin incorporation on microstructure of *ZnS* is not available. This was the key motivation behind this work. In the present study we report the synthesis of *ZnS* and *Sn* doped *ZnS* thin films by CBD and their microstructural and optical properties.

2. Experimental

ZnS and *Sn* doped *ZnS* thin film was deposited on well treated microscope glass slide substrates as substrate treatment plays an important role in deposition of thin film by CBD process. The substrate cleaning steps involved overnight keeping in chromic acid followed by rinsing in distil water and ultrasonic cleaning in equivolume acetone and alcohol for about 20 minutes. The glass substrates were lightly rubbed before immersion for better adherence and dipped vertically in the bath solution. All the chemicals and reagents used to prepare the reacting bath were of analytical reagent grade. 80 ml 0.2 M zinc acetate [$Zn(CH_3COO)_2.2H_2O$] and 160 ml 0.2 M thiourea [$(NH_2)_2CS$] was added and stirred properly at room temperature. Then 0.66 M tri-sodium citrate as complexing agent was mixed properly in the solution. After that, ammonia solution was added to make the pH 11 of the bath. The substrates were immersed in the bath solution for 24 hours and a white colored film with a faint shadow of blue appears over the surface of the substrate. To obtained *Sn* doped *ZnS* thin film, 0.1 M tin chloride ($SnCl_2$, $2H_2O$) was added in proper ratio with the solution. In this process *ZnS*, 2.5% *Sn: ZnS* and 5% *Sn: ZnS* thin films were prepared. Attempts to prepare films with more than 5% resulted in instability of the acetate bath resulting in non-uniform films with pinholes. Film thickness measured using gravimetric weight difference method[22-23] was approximately ~1300 nm for *ZnS* and ~1400 nm for 5% *Sn: ZnS*.

The phase identification and crystalline properties of undoped and doped samples were studied by X-ray diffraction (XRD) method employing a Bruker (D8 advance) x-ray diffractometer with Ni-filtered CuK_α radiation (λ=1.5418 Å). Reitveld analysis was done to obtain microstructural information by using MAUD 2.33 software, which is specially designed to simultaneously refine both the structural and microstructural parameters through a least squares method[24-25].The Transmission electron microscopy (TEM) investigation was carried out using Tecnai F30 G^2, FEI, Hillsboro, Oregon microscope operating at 200 kV accelerating voltage. SAED pattern was analyzed to get detail information about structure and TEM was used for particle size estimation. The sample was separated from the substrate carefully and dispersed in ethanol by ultrasonication process. Then they were mounted on a carbon coated copper grid, dried, and used for TEM measurements. Energy dispersive X-ray (EDX) analyses were carried out to qualitatively measure the sample stoichiometry of films. The optical absorption measurements were carried out using a Schimatzu dual beam UV-Vis spectrophotometer (Model No: UV-1800). The spectrum was recorded by using a similar glass slide as reference and hence the absorption due to the film only was obtained. The band gap of the films was calculated from the absorption edge of the spectrum.

3. Results and discussions

The X-ray diffraction patterns of undoped *ZnS* and *Sn* doped *ZnS* films are shown in Figure 1. The diffraction pattern for undoped *ZnS* is shown in Figure 1 (a). Figure 1 (b) and 1 (c) shows the diffractograms for 2% and 5% *Sn: ZnS* films respectively. The materials were scanned in the range 20-70°. Intensity in arbitrary units is plotted against 2θ in Figure 1. It is seen from Figure 1 (a) that peaks appears at 26.42°, 28.38°, 30.35° and 47.65° respectively. The diffractogram of the sample reveals that all the peaks are in good agreement with the Joint committee on powder diffraction standard (JCPDS) data belonging to hexagonal *ZnS* structure (Card No. 36-1450). The corresponding reflecting planes are (100), (002), (101) and (110) respectively. The (101) peak appears with maximum intensity at 30.35°. The major peak along with the other peaks is shifted slightly towards lower angles for tin doped films. The peak positions for 5% *Sn: ZnS* films are 26.32°, 28.3°, 30.20° and 47.50° respectively. This might be due to the replacement of smaller Zn^{2+} ions (0.74 Å) by the bigger Sn^{2+} ions (0.99 Å). Apart from *ZnS* characteristic peaks, no extra peaks due to tin their complex oxides could be detected. This observation suggests that the films are single phase and tin ion might have substituted *Zn* site without changing the hexagonal structure. In hexagonal wurtzite structure (100) plane appears with maximum intensity and (101) is the second highest intensity peak (JCPDS 36-1450). In our case (101) plane appears with maximum intensity indicating preferred orientation along (101). However the relative intensity of the major diffraction peak corresponding to hexagonal wurtzite structure (101 diffraction plane) increases with respect to the other peaks with increasing tin incorporation. In other words, the ratio I_{100} / I_{101} increases with increasing tin incorporation indicating the structure gets more ordered. For pure *ZnS* film, the ratio is ~0.32 and it increases to ~0.79 for 5% *Sn: ZnS*. Such enhanced ordering of structure possibly also facilitates film growth rate and enhanced thickness due to tin doping.

The Rietveld output *ZnS* is shown in Figure 2. Figure 2 shows the typical Rietveld fitting output with the difference plot i.e. the residual of fitting between the observed pattern and fitted pattern at the bottom. The dotted curve is the experimental plot and the continuous line is the fitted output of Rietveld analysis. An appropriate fit (continuous line) has been observed with the goodness of fit (GOF) value ~1.3 indicating a good quality of fitting within the admissible range[26]. The values

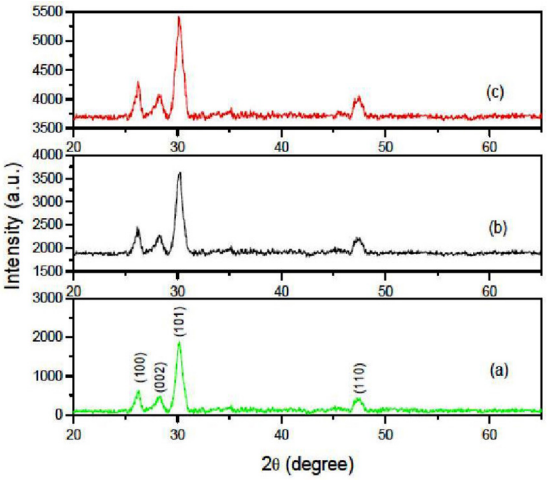

Figure 1: X-ray diffraction pattern of (a) *ZnS*, (b) 2.5% *Sn: ZnS* and (c) 5% *Sn: ZnS.*

of lattice parameters obtained from Rietveld refinement are $a = b = 3.872 \pm 0.000757$ Å and $c = 6.290 \pm 0.00317$ Å. The corresponding values for 2.5% *Sn: ZnS* are 3.895 ± 0.00082 Å and 6.263 ± 0.00281 Å respectively while they are 3.943 ± 0.001Å and 6.269 ± 0.0033 Å respectively for 5% *Sn: ZnS*. The average value of particle size estimated from Rietveld refinement using MAUD software are ~12.51 nm, ~11.92 nm and ~10.61 nm for *ZnS*, 2.5% *Sn: ZnS* and 5% *Sn: ZnS* sample respectively. Thus a reduction of particle size was observed due to tin doping. The microstrain (ε)in the films increased due to tin incorporation. The value of average microstrain enhanced from $\sim 2.787 \times 10^{-3}$ for *ZnS* to $\sim 2.971 \times 10^{-3}$ for 5% *Sn: ZnS*.The decrease in average particle size might be due tothe enhancement of strain in the film. Similar effects of decrease of particle size with increasing strain have been reported for Cd doping in ZnO thin film [27]. As explained in some literature, such increase in strain energy may lead to enhanced polycrystallinity[22,28] i.e. reduction of particle size.

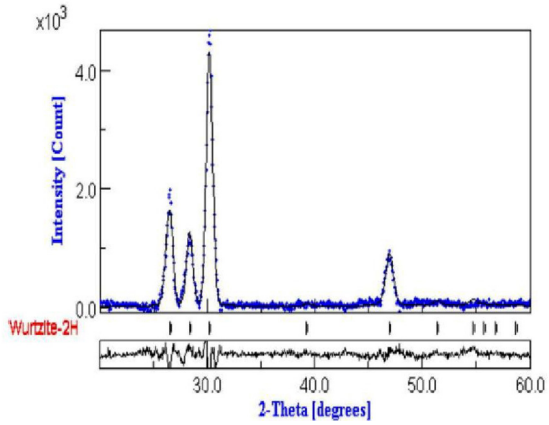

Figure 2: Reitveld output of *ZnS* [experimental (dotted) and fitted (continuous)].

The indexed selected area electron diffraction (SAED) pattern of undoped *ZnS* is shown in Figure 3 (a). The observed diffraction planes are (100), (002), (101), (110) and (112) respectively. These are accordance with the result obtained from XRD data and confirm the presence of hexagonal phase. The *d* value of ~3.32 Å in the HRTEM image (Figure 3b) for observed lattice fringe (region 1) for the first diffraction ring corresponding to (100) plane compares well with JCPDS data. The region 2 shows two planes (100) and (101) overlap each other. The particle size obtained from the TEM image is around 12-20 nm as shown in Figure 3(c). A histogram is plotted (Figure 3(d)) to get the idea about the distribution of particle size. Most of the particles are distributed in the range 14-18 nm. Average value of the particle size is about 16.5 nm which compares well with x-ray value of ~12.51 nm.

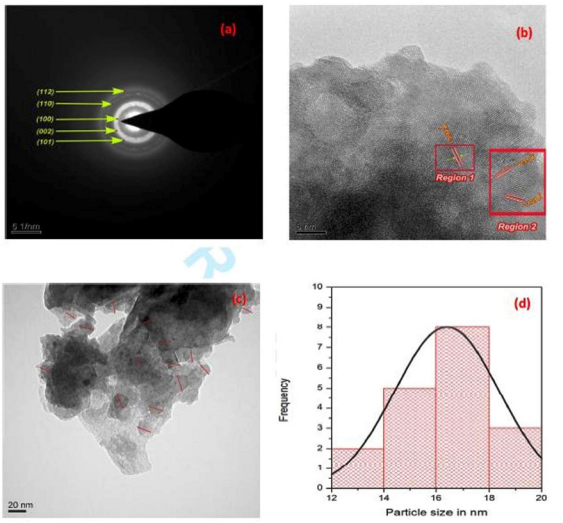

Figure 3. (a) Selected area electron diffraction (SAED) image of *ZnS*; (b) HRTEM image showing inter-planar distances d_{100} and d_{101} of hexagonal *ZnS*; (c) TEM image showing nanometer size particles of *ZnS*; and (d) histogram of particle size distribution.

FESEM micrographs of *ZnS* and 5% *Sn: ZnS* is shown is Figures 4(a) and 4(b) respectively. Uniform and good surface morphology can be concluded from FESEM images. Agglomeration of small crystallites is found to be present in certain regions on the film surface indicating that the particles formed cluster over the glass substrate during chemical bath deposition process. There are also some holes between the particles indicating porosity of the obtained films. No significant change in surface morphology is observed due to tin doping.

Although no compositional analysis was attempted in the present study, the incorporation of *Sn* in the films was verified by the EDAX result. Figure 5 shows the energy dispersive X-ray spectrum of 5% *Sn: ZnS* film. The spectrum reveals the presence of *Zn*, *S* and *Sn* elements in the deposited film. The silicon and oxygen signal appears from the substrate. Trace amount of carbon impurity was detected in the film

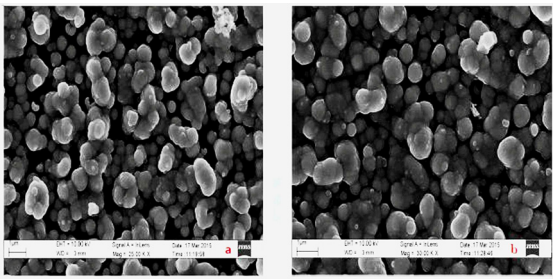

Figure 4: FESEM image of (a) *ZnS* and (b) 5% *Sn: ZnS*.

which appears possibly from zinc acetate and/or thiourea used during bath preparation.

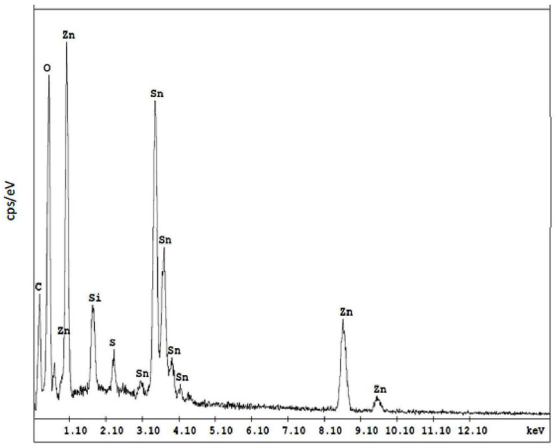

Figure 5: EDX pattern of 5% *Sn: ZnS*.

Figure 6 shows optical absorbance spectrum [absorbance (A) as a function of wavelength (λ)] for *ZnS* and *Sn* doped *ZnS* films. The absorbance coefficient increases with increasing *Sn* doping for the entire wavelength range. Increase of absorbance implies decrease of transmittance which might be due to enhanced thickness due to *Sn* incorporation. This might be attributed to increase of film thickness due to tin enrichment. Although no systematic thickness measurement was carried out in our work, a rough and ready gravimetric technique (measuring the weight change of the substrate due to film deposition and dividing this by area of film deposition and known density of the material) shows increase of thickness with tin enrichment (~1300 nm for pure *ZnS* to ~1400 nm for highest tin content film).Band gap energy (E_g) was derived from the mathematical treatment of the data obtained from the absorbance vs. wavelength spectrum for direct band gap *ZnS*[29] using Tauc's relationship[30]:

$$(\alpha h\nu)^2 = A(h\nu - E_g)$$

where v is the photon frequency, A is a function of index of refraction and hole/electron effective masses and h is the Planck's constant. Absorption coefficient (α) was evaluated

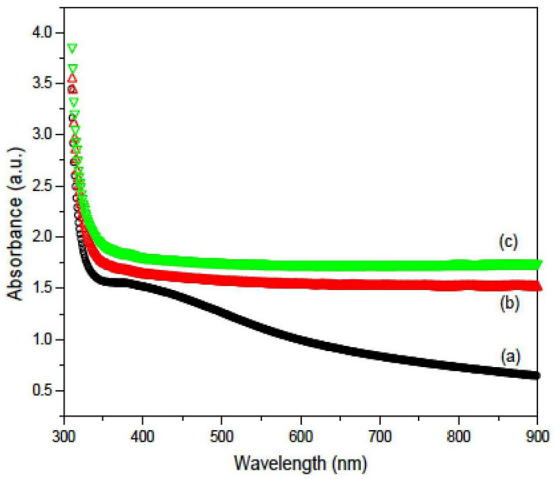

Figure 6: Absorbance versus photon wavelength for (a) *ZnS*, (b) 2.5% *Sn: ZnS* and (c) 5% *Sn: ZnS*.

from the relation $A = 2.303\alpha t$ and using the measured values of thicknesses (t) for *ZnS* and *Sn* doped *ZnS* films. Figure 7 shows the plot of $(\alpha h\nu)^2$ as a function of photon energy $h\nu$. Extrapolation of the line to the base line, where the value of $(\alpha h\nu)^2$ is zero, gives band gap E_g. The sharp absorption edge corresponding to the band gap confirms the good quality of the films. The band gap energy increases from ~3.69 eV for *ZnS* to ~ 3.90 eV for 5% *Sn: ZnS* indicating a blue shift. Incidentally the band gap of tin sulphide is much lower than that of zinc sulphide and thus incorporation of tin should have caused red shift in band gap. Thus it appears that a particle size reduction of ~15% only cannot lead to such enhancement in band gap. Since the particle sizes observed are much higher than the *ZnS* Bohr exciton radius, quantum confinement effect is obviously not the reason behind such a blue shift. The only other possible reason might be enhancement of relative intensity of the major diffraction peak corresponding to hexagonal wurtzite structure (100 plane). Such enhancement of relative intensity implies more ordered structure and a band gap closer to bulk value[3]. Nasr et al[3] observed such ordering due to pH variation of the reactants. In our case, we get it as a result of enhanced tin incorporation. Thus the enhancement in band gap may be ascribed enhancement of structure ordering resulting from enhancement of relative intensity of the major diffraction peak of hexagonal wurtzite structure. In hexagonal wurtzite structure, the band gap can even reach a very high value of ~4.4 eV[31].

Dependence of photoluminescence (PL) spectra of *ZnS* films on the excitation wavelength (λ_{ex}) has been investigated. Figure 8 shows the PL intensity spectrum is plotted against wavelength for different excitation wavelength (340-420 nm). A redshift has been observed with increase of excitation wavelength which may be due to different contribution of excitonic emissions and their phonon replicas[32]. The intensity of the peaks decreases with excitation wavelength.

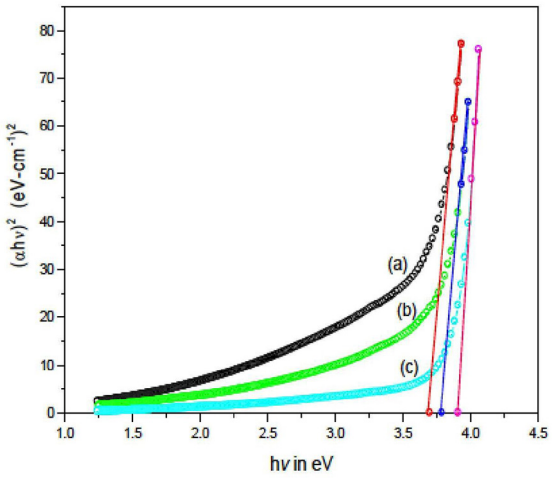

Figure 7: Plot of $(\alpha h\nu)^2$ versus $h\nu$ for (a) *ZnS*, (b) 2.5% *Sn*: *ZnS* and (c) 5% *Sn*: *ZnS*.

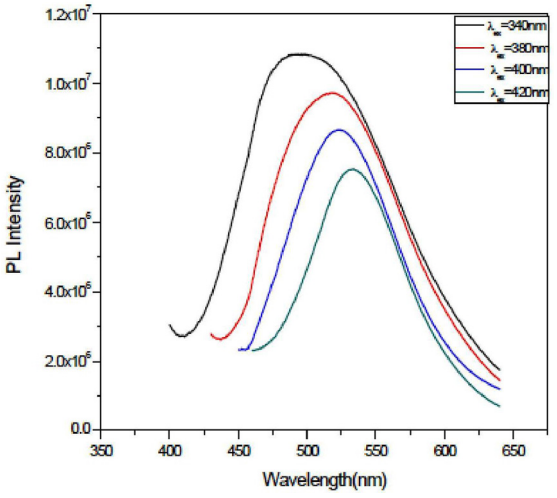

Figure 8: PL spectrum of *ZnS* film for different excitation wavelengths.

4. Conclusion

The primary aim of the present investigation was to explore the possibility of doping *ZnS* with tin by CBD method. *Sn* doped *ZnS* films with different percentage of *Sn* content (2.5% and 5%) could be successfully synthesized through this technique for the first time to the best of our knowledge. The films had good adherence to the substrate. Apart from being an inexpensive and simple technique, the method uses milder reaction conditions than those employed by most chemical methods proposed in the literature. Particle size evaluated using Reitveld technique using MAUD software a constantly decreasing trend with increasing tin incorporation. The average particle size of ~12.51 nm for *ZnS* evaluated by X-ray technique is on the lower side compared to TEM observation (~16.5 nm). The crystal structure is hexagonal as confirmed by XRD and TEM. SAED patterns reveals the presence of (100),(002), (101) and (110) hexagonal planes. The major peak along with the other peaks is shifted slightly towards lower angles for tin doped films. This observation along with EDX observation confirms the replacement of zinc ion by tin ions in the *ZnS* lattice. *Sn* doping increases the fundamental absorption edge. The band gap energy increases from ~ 3.69 eV for *ZnS* to ~ 3.90 eV for 5% *Sn: ZnS*. Such enhancement of bandgap might be due to enhancement of relative intensity of the major diffraction peak (100) corresponding to hexagonal wurtzite structure consequently leasing to a more ordered structure. The materials are therefore useful for configurations that involve bandgap engineering.

5. Acknowledgement

Theauthors acknowledge the instrumental support from DST (Govt. of India) under departmental FIST programme (Grant No. SR/FST/PS-II-001/2011). The authors also acknowledge Dr. M. Fu, School of Materials Science and Engineering, North West Polytechnical University, Xi'an, Shannxi, China for recording the TEM images.

6. References

1. Ozutok F, Erturk E, Bilgin V. Growth, Electrical, and Optical Study of ZnS:Mn Thin Films. *Acta Physica Polonica A*. 2012;121(1):221-223. DOI: 10.12693/APhysPolA.121.221

2. Rawlins TGR, Woodward RJ. Sputtered zinc sulphide films on silicon. *Journal of Materials Science*. 1972;7(3):257-264. DOI: 10.1007/BF00555626

3. Nasr TB, Kamoun N, Kanzari M, Bennaceur R. Effect of pH on the properties of ZnS thin films grown by chemical bath deposition. *Thin Solid Films*. 2006;500(1-2):4-8. DOI: 10.1016/j.tsf.2005.11.030

4. Shinde MS, Ahirrao PB, Patil IJ, Patil RS. Studies on nanocrystalline ZnS thin films prepared by modified chemical bath deposition method. *Indian Journal of Pure & Applied Physics*. 2011;49(11):765-768.

5. Thi TM, Hien NT, Thu DX, Trung VQ. Thin films containing Mn-doped ZnS nanocrystals synthesised by chemical method and study of some of their optical properties. *Journal of Experimental Nanoscience*. 2012;8(5):694-702. DOI: 10.1080/17458080.2011.599045

6. Hachiya S, Shen Q, Toyada T. Effect of ZnS coatings on the enhancement of the photovoltaic properties of PbS quantum dot-sensitized solar cells. *Journal of Applied Physics*. 2012;111(10):104315. DOI: 10.1063/1.4720468

7. Tec-Yam S, Rojas J, Rejón V, Oliva AI. High quality antireflective ZnS thin films prepared by chemical bath deposition. *Materials Chemistry and Physics*. 2012;136(2-3):386-393. DOI: 10.1016/j.matchemphys.2012.06.063

8. Pawar MJ, Nimkar SD, Nandurkar PP, Tale AS, Deshmukh SB, Chaure SS. Effect of Sn^{2+} Doping on Optical Properties of Thiourea Capped ZnS Nanoparticles. *Chalcogenide Letters*. 2010;7(2):139-143.

9. Baranski AS, Bennet MS, Fawcett WR. The physical properties of CdS thin films electrodeposited from aqueous diethylene glycol solutions. *Journal of Applied Physics*. 1983;54(11):6390-6394. DOI: 10.1063/1.331916

10. Turan E, Zor M, Aybek AS, Kul M. Electrical properties of ZnO/Au/ZnS/Au films deposited by ultrasonic spray pyrolysis. *Thin Solid Films*. 2007;515(24):8752-8755. DOI: 10.1016/j.tsf.2007.04.001

11. Daranfed W, Aida MS, Hafdallah A, Lekiket H. Substrate temperature influence on ZnS thin films prepared by ultrasonic spray. *Thin Solid Films*. 2009;518(4):1082-1084. DOI: 10.1016/j.tsf.2009.03.227

12. Ubale AU, Kulkarni DK. Preparation and study of thickness dependent electrical characteristics of zinc sulfide thin films. *Bulletin of Materials Science*. 2005;28(1):43-47. DOI: 10.1007/BF02711171

13. Goudarzi A, Aval GM, Sahraei R, Ahmadpoor H. Ammonia-free chemical bath deposition of nanocrystalline ZnS thin film buffer layer for solar cells. *Thin Solid Films*. 2008;516(15):4953-4957. DOI: 10.1016/j.tsf.2007.09.051

14. Gayou VL, Salazar-Hernandez B, Constantino ME, Andrés ER, Díaz T, Macuil RD, et al. Structural studies of ZnS thin films grown on GaAs by RF magnetron sputtering. *Vacuum*. 2010;84(10):1191-1194. DOI: 10.1016/j.vacuum.2009.10.023

15. Agawane GL, Shin SW, Moholkar AV, Gurav KV, Yun JH, Lee JY, et al. Non-toxic complexing agent Tri-sodium citrate's effect on chemical bath deposited ZnS thin films and its growth mechanism. *Journal of Alloys and Compounds*. 2012;535:53-61. DOI: 10.1016/j.jallcom.2012.04.073

16. Öztaş M, Bedir M, Yazici AN, Kafadar EV, Toktamış H. Characterization of copper-doped sprayed ZnS thin films. *Physica B: Condensed Matter*. 2006;381(1-2):40-46. DOI: 10.1016/j.physb.2005.12.248

17. Ortíz-Ramos DE, González LA, Ramirez-Bon R. p-Type transparent Cu doped ZnS thin films by the chemical bath deposition method. *Materials Letters*. 2014;124:267-270. DOI: 10.1016/j.matlet.2014.03.082

18. Peng WG, Cong GW, Qu SC, Wang ZG. Synthesis and photoluminescence of ZnS:Cu nanoparticles. *Optical Materials*. 2006;29(2-3):313-317. DOI: 10.1016/j.optmat.2005.10.003

19. Goudarzi A, Aval GM, Park SS, Choi M, Sahraei R, Ullah MH, et al. Low-Temperature Growth of Nanocrystalline Mn-Doped ZnS Thin Films Prepared by Chemical Bath Deposition and Optical Properties. *Chemistry of Materials*. 2009;21(12):2375-2385. DOI**:** 10.1021/cm803329w

20. Maity R, Chattopadhyay KK. Synthesis and optical characterization of ZnS and ZnS:Mn nanocrystalline thin films by chemical route. *Nanotechnology.* 2004;15(7):812-816. DOI: 10.1088/0957-4484/15/7/017

21. Ummartyotin S, Bunnak N, Juntaro J, Sain M, Manuspiya H. Synthesis and luminescence properties of ZnS and metal (Mn, Cu)-doped-ZnS ceramic powder. *Solid State Sciences*. 2012;14(3):299-304. DOI: 10.1016/j.solidstatesciences.2011.12.005

22. Mondal S, Mitra P. Preparation of cadmium-doped ZnO thin films by SILAR and their characterization. *Bulletin of Materials Science*. 2012;35(5):751-757. DOI: 10.1007/s12034-012-0350-2

23. Kale SS, Mane RS, Pathan HM, Shaikh AV, Joo OS, Han SH. Preparation and characterization of ZnTe thin films by SILAR method. *Applied Surface Science*. 2007;253(9):4335-4337. DOI: 10.1016/j.apsusc.2006.09.043

24. Rietveld HM. A profile refinement method for nuclear and magnetic structures. *Journal of Applied Crystallography*. 1969;2:65-71. DOI: 10.1107/S0021889869006558

25. Datta A, Pal M, Chakravorty D, Das D, Chintalpudi SN. Disorder in Ni_3Fe. *Journal of Magnetism and Magnetic Materials*. 1999;205(2-3):301-306. DOI: 10.1016/S0304-8853(99)00498-9

26. Pal M, Das D, Chintalpudi SN, Chakravorty D. Preparation of nanocomposites containing iron and nickel-zinc ferrite. *Journal of Materials Research*. 2000;15(3):683-688. DOI: 10.1557/JMR.2000.0101

27. Maiti UN, Ghosh PK, Ahmed SF, Mitra MK, Chattopadhyay KK. Structural, optical and photoelectron spectroscopic studies of nano/micro ZnO:Cd rods synthesized via sol-gel route. *Journal of Sol-Gel Science and Technology*. 2007;41(1):87-92. DOI: 10.1007/s10971-006-0116-7

28. Lee YE, Kim YJ, Kim HJ. Thickness dependence of microstructural evolution of ZnO films deposited by rf magnetron sputtering. *Journal of Materials Research*. 1998;13(5):1260-1265. DOI: 10.1557/JMR.1998.0180

29. Allouche NK, Nasr TB, Kamoun NK, Guasch C. Synthesis and properties of chemical bath deposited ZnS multilayer films. *Materials Chemistry and Physics*. 2010;123(2-3):620-624. DOI: 10.1016/j.matchemphys.2010.05.026

30. Tauc J, ed. *Amorphous and Liquid Semiconductor*. New York: Plenum Publishing; 1974. 441 p. DOI: 10.1007/978-1-4615-8705-7

31. Ghosh PK, Jana S, Nandy S, Chattopadhyay KK. Size-dependent optical and dielectric properties of nanocrystalline ZnS thin films synthesized via rf-magnetron sputtering technique. *Material Research Bulletin*. 2007;42(3):505-514. DOI: 10.1016/j.materresbull.2006.06.019

32. Khan F, Ameen S, Song M, Shin HS. Influence of excitation wavelength on photoluminescence spectra of Al doped ZnO films. *Journal of Luminescence.* 2013;134:160-164. DOI: 10.1016/j.jlumin.2012.08.054